



## Competing influence of damage buildup and lattice vibrations on ion range profiles in Si

M. Posselt, M. Mäder, R. Grötzschel, and M. Behar

Citation: [Applied Physics Letters](#) **83**, 545 (2003); doi: 10.1063/1.1594281

View online: <http://dx.doi.org/10.1063/1.1594281>

View Table of Contents: <http://scitation.aip.org/content/aip/journal/apl/83/3?ver=pdfcov>

Published by the [AIP Publishing](#)

---

### Articles you may be interested in

[Structural characterization and modeling of damage accumulation in In implanted Si](#)

*J. Appl. Phys.* **95**, 150 (2004); 10.1063/1.1631076

[Influence of in situ ultrasound treatment during ion implantation on amorphization and junction formation in silicon](#)

*J. Vac. Sci. Technol. B* **20**, 1448 (2002); 10.1116/1.1493784

[Characterization by medium energy ion scattering of damage and dopant profiles produced by ultrashallow B and As implants into Si at different temperatures](#)

*J. Vac. Sci. Technol. B* **20**, 974 (2002); 10.1116/1.1477420

[High-energy ion-implantation-induced gettering of copper in silicon beyond the projected ion range: The trans-projected-range effect](#)

*J. Appl. Phys.* **88**, 5645 (2000); 10.1063/1.1316054

[Copper gettering at half the projected ion range induced by low-energy channeling He implantation into silicon](#)

*Appl. Phys. Lett.* **77**, 972 (2000); 10.1063/1.1289062

---

The image shows the cover of an Applied Physics Reviews journal issue. It features a blue and orange color scheme with a molecular structure background. The text 'NEW Special Topic Sections' is prominently displayed in white. Below it, 'NOW ONLINE' is written in yellow, followed by the title 'Lithium Niobate Properties and Applications: Reviews of Emerging Trends' in white. The AIP Applied Physics Reviews logo is in the bottom right corner.

**NEW Special Topic Sections**

**NOW ONLINE**  
Lithium Niobate Properties and Applications:  
Reviews of Emerging Trends

**AIP** Applied Physics Reviews

## Competing influence of damage buildup and lattice vibrations on ion range profiles in Si

M. Posselt,<sup>a)</sup> M. Mäder, and R. Grötzschel

*Forschungszentrum Rossendorf, Institute of Ion Beam Physics and Materials Research, P.O. Box 510119, D-01314 Dresden, Germany*

M. Behar

*Instituto de Fisica, P.O. Box 15051, 91501-970 Porto Alegre, Brazil*

(Received 10 December 2002; accepted 22 May 2003)

Phosphorus depth profiles in Si obtained by 140 keV implantation in the [001] axial channel direction and in a direction  $7^\circ$  off axis are investigated at two different doses ( $5 \times 10^{13}$  and  $5 \times 10^{15}$  cm<sup>-2</sup>) for implantation temperatures of 350 °C and room temperature (RT). At low dose and at channeling incidence, the penetration depth of implanted ions is higher at RT than at 350 °C. This behavior is caused by the dechanneling of lattice vibrations. At high dose, the temperature dependence of the shape of the implantation profile is opposite that at low dose, due to enhanced dechanneling by defect accumulation at RT. On the other hand, damage buildup does not occur at elevated temperature. The temperature dependence of the profiles obtained by tilted implantation is much less than for the channeled implants. The P profiles measured can be reproduced very well by atomistic simulations which take into account both lattice vibrations and defect accumulation during ion bombardment. © 2003 American Institute of Physics. [DOI: 10.1063/1.1594281]

For many years it has been known that channeling effects influence the shape of ion range distributions obtained by implantation into single crystalline silicon.<sup>1-6</sup> The orientation of the ion beam relative to the crystal axes determines the fraction of incident ions that moves initially within axial or planar channels. However, motion of energetic projectiles in the crystal is not only influenced by the geometrical arrangement of the lattice sites but also by thermal vibrations of the atoms and the buildup of radiation damage during implantation. This may lead to both dechanneling and rechanneling of the implanted ions. Therefore, at a given implantation energy the shape of the ion range profiles may depend on the following implantation parameters: implantation temperature, dose, and dose rate. In silicon device manufacturing these parameters must be accurately controlled in order to obtain reproducible electrical dopant profiles.<sup>7</sup> The present work reports on a detailed study on the competing influence of temperature and dose on the shape of as-implanted depth profiles of phosphorus. The experimental results are not only interpreted qualitatively, they can also be reproduced quantitatively by atomistic computer simulations.

Phosphorus ions were implanted into a *p*-type (001) Si substrate at 140 keV at doses of about  $5 \times 10^{13}$  and  $5 \times 10^{15}$  cm<sup>-2</sup> at a dose rate of about  $5 \times 10^{11}$  cm<sup>-2</sup> s<sup>-1</sup>. The exact values of the doses implanted are given in Figs. 1 and 2. Implantations in both the [001] axial channel direction and in a direction  $7^\circ$  off axis were performed. The ion beam was aligned in the [001] direction prior to implantation by a standard procedure employed in channeling Rutherford backscattering spectrometry (RBS/C).<sup>8</sup> For the nonchanneled low dose implants, the  $7^\circ$  tilt angle with respect to [001] and the  $22.5^\circ$  rotation angle relative to [110] were set using the five-axis goniometer that was employed for beam alignment for

[001] channeling implantation. The high dose implant was performed using the standard implanter setup for  $7^\circ$  tilted implantations. The implantations were carried out at room temperature (RT) as well as at elevated temperatures (300 and 350 °C). The temperature was controlled by a thermocouple. For the high temperature implants a BORALECTRIC® heater was used. After implantation, RBS/C analysis was performed to obtain information about as-implanted damage. The phosphorus depth profiles were measured by secondary ion mass spectrometry (SIMS) at Evans East (East Windsor, NJ) using a Phi quadrupole SIMS instrument. The P detection limit in Si was  $1 \times 10^{15}$  cm<sup>-3</sup>. The accuracy of the depth calibration was 5%–10%.

The thick lines in Figs. 1(a) and 1(b) depict the SIMS data for the low dose implants at RT and at 350 °C, respectively. A comparison of Figs. 1(a) and 1(b) shows that the shape of the phosphorus profiles obtained by channeling implantation is strongly dependent on the temperature. The profiles of the tilted implants are nearly independent of the temperature. At implantation dose of about  $5 \times 10^{13}$  cm<sup>-2</sup>, the accumulation of radiation defects is small so it should not cause much dechanneling of the incident ions. Therefore, the temperature dependence observed for the channeling implantation profiles is solely attributed to thermal vibrations whose dechanneling effect is considerably stronger at 350 °C [Fig. 1(b)] than at RT [Fig. 1(a)].

The phosphorus profiles obtained by the high dose implantation at RT and at elevated temperatures (300 and 350 °C) are depicted in Figs. 2(a) and 2(b), respectively. Again, a significant dependence of the shape of the phosphorus profiles on the temperature is found. However, this dependence is opposite that observed in Fig. 1 for the low dose implant. This can be explained as follows. For the RT implant [Fig. 2(a)], the damage buildup during ion bombardment causes strong dechanneling of the incident ions. Therefore, the shape of the channeling implantation profile differs

<sup>a)</sup>Author to whom correspondence should be addressed; electronic mail: m.posselt@fz-rossendorf.de

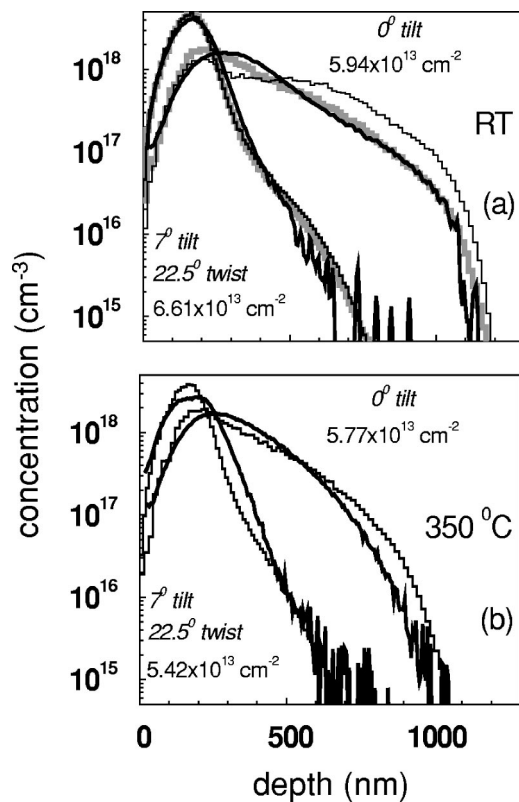


FIG. 1. P depth profiles obtained by 140 keV implantation into (001) Si at a dose of about  $5 \times 10^{13} \text{ cm}^{-2}$ , at RT (a) and at  $350 \text{ }^\circ\text{C}$  (b). The exact doses are shown. Two orientations of the ion beam were considered: (i) parallel to the [001] channel direction and (ii)  $7^\circ$  off this direction. In the second case, the angle between the projection of the beam direction on the (001) plane and the [110] direction was  $22.5^\circ$ . The depth axis is parallel to [001]. The profiles depicted by thick lines were measured by SIMS at Evans East, East Windsor, NJ. The histograms show results of atomistic simulations that do not (black) and do (gray) consider damage buildup during implantation.

greatly from that shown in Fig. 1(a). In the case of the tilted implant, the channeling tail is not as pronounced as it is in Fig. 1(a) since ion-beam-induced defect accumulation also prevents rechanneling. RBS/C measurements show that in both channeling and tilted implantations an amorphous layer about 280 nm thick formed. It should be noted, however, that this layer is not the main cause of the alteration in profile shape, it is the damage buildup below the amorphization threshold.<sup>6</sup>

The shapes of the phosphorus profiles shown in Figs. 1(b) and 2(b) are rather similar. Obviously, at elevated temperatures the accumulation of defects which are relevant for dechanneling of the implanted ions is very small, in contrast to RT implantations. Therefore, at 300 and  $350 \text{ }^\circ\text{C}$ , these defects formed by previous ion impact should largely have disappeared before a subsequently implanted ion hits the same region of the target. The period between consecutive ion impacts in a target region where the amount of nuclear energy deposition (or displacements per atom) is larger than a critical value can be roughly estimated in the following manner. Assuming that the cascade region of a single ion impact can be modeled by a cylindrical track,<sup>9</sup> the lateral cross section  $\sigma_0$  of this region can be calculated using

$$\sigma_0 = \frac{S_n}{E_c} \quad (1)$$

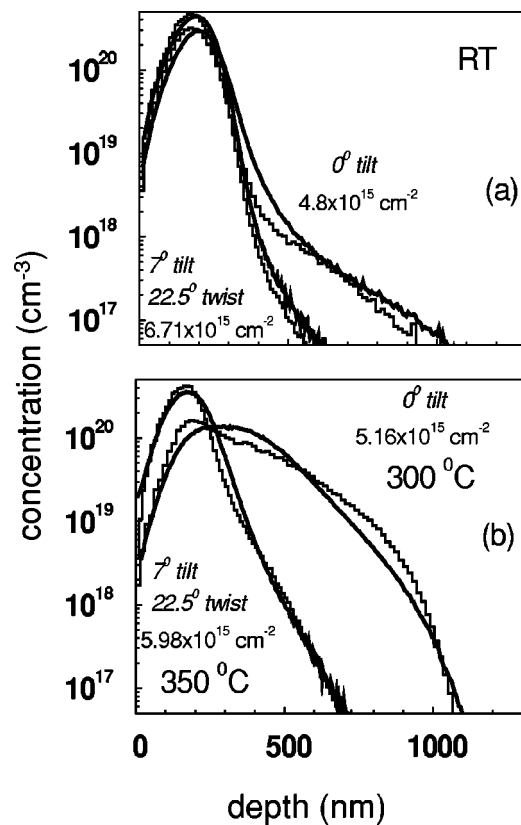


FIG. 2. Phosphorus depth distributions for 140 keV implantation at a dose of about  $5 \times 10^{15} \text{ cm}^{-2}$ . Thick lines and histograms depict SIMS data and the results of computer simulations, respectively. Similar to in Fig. 1, the results of channelled and tilted implantations at RT (a) and at elevated temperature (b) are shown. At RT, both the channelled and the tilted implantation led to amorphization. The thickness of the amorphous layer determined by RBS/C is 280 nm. The simulations yielded a thickness of 278 nm.

$S_n$  is the nuclear stopping cross section of the ion in the target. The critical nuclear energy deposition per atom for defect production,  $E_c$ , should be somewhat lower than the displacement energy for Frenkel pair generation,  $E_d$ , in a virgin silicon crystal, since most atomic displacements occur in the region of a collision cascade where the target structure is no longer perfect. In the case of 140 keV phosphorus implantation, the use of the universal nuclear stopping cross section,<sup>10</sup> and assuming  $E_c = 0.25E_d$  ( $E_d = 15 \text{ eV}$ ), leads to a lateral cross section  $\sigma_0$  of about  $1 \text{ nm}^2$ . Therefore, at a dose rate of  $5 \times 10^{11} \text{ cm}^{-2} \text{ s}^{-1}$ , the time between consecutive ion impacts in a damaged region is of the order of 100 s. Together with previous considerations, this means that at 300 and  $350 \text{ }^\circ\text{C}$  the lifetime of defects for dechanneling is smaller than this period.

Atomistic computer simulations showed that the as-implanted defect structure consists of a variety of defect species.<sup>11,12</sup> Many single vacancies and self-interstitials as well as a certain percentage of complex defects that contain tens to hundreds of atoms form. The latter may be considered as the defects mainly responsible for dechanneling of the implanted ions.<sup>6</sup> The simulations demonstrated that such complex defects shrink considerably at a few  $100 \text{ }^\circ\text{C}$ ,<sup>11</sup> within 1 ns of their formation. This is consistent with the present experimental results.

The measured P depth distributions were simulated using the Crystal-TRIM program which is described in detail

elsewhere.<sup>6,13–15</sup> This code treats the motion of implanted ions in the target material within the framework of binary collision approximation, i.e., by the consideration of a sequence of binary collisions with target atoms in close vicinity to the ion trajectory. The black histograms in Fig. 1 show the results obtained for the low dose implant at RT and at 350 °C. The agreement with the experimental data is good. In the simulations, the target was assumed to consist of a perfect Si crystal with a native SiO<sub>2</sub> surface layer 1.5 nm thick. The following values were used for parameters  $C_\lambda$  and  $C_{el}$  in the model for the electronic energy loss of an incident ion in a collision with a target atom:<sup>13,14</sup>  $C_\lambda=1.0$  and  $C_{el}=1.38$ . The first parameter was employed to calculate the electronic energy loss averaged over all impact parameters using the electronic stopping cross section given in Ref. 10. The second parameter describes the impact-parameter dependence of electronic energy loss in the modified Oen–Robinson model.<sup>13,14,16</sup> Thermal vibrations of the lattice atoms were treated as follows. Since the time of binary projectile–target collision is generally much shorter than the period of thermal vibration of a lattice atom, it suffices to consider the instantaneous thermal displacement of the atom. It is assumed to obey a Gaussian distribution with a root mean square (rms)  $\langle u^2 \rangle^{1/2}$  obtained by the Debye model<sup>17</sup>

$$p(x) = \frac{1}{(2\pi\langle u^2 \rangle)^{1/2}} \exp\left(-\frac{x^2}{2\langle u^2 \rangle}\right), \quad (2)$$

$$\langle u^2 \rangle^{1/2} = \frac{12.06 \text{ \AA}}{((T_D/K)(M_t/\text{amu}))^{1/2}} \times \left( \frac{1}{4} + \frac{1}{y^2} \int_0^y \frac{z dz}{\exp(z) - 1} \right)^{1/2}, \quad y = \frac{T_D}{T},$$

where  $M_t$  is the mass of a target atom.  $T_D$  and  $T$  are the Debye temperature and the actual temperature of the target, respectively. In the Crystal-TRIM code a Debye temperature of 500 K is used. This value is in agreement with results of precise channeling radiation measurements of thermal vibrational amplitudes<sup>18,19</sup> The formula for the rms of thermal displacements shows that the temperature dependence of this quantity is particularly pronounced if the Debye temperature is relatively low, like in the case of silicon. For example, if under otherwise identical conditions a silicon carbide target with  $T_D=1120$  K were to be used in low dose P implantation, the temperature dependence of the profile shape would be much smaller than that in the case of Si.

Atomistic computer simulations were also performed for the high dose (about  $5 \times 10^{15} \text{ cm}^{-2}$ ) implants. In Fig. 2 the histograms show the results. In order to describe the accumulation of defects which are relevant for dechanneling of the implanted ions, a known phenomenological model for damage buildup, elucidated, e.g., in Ref. 20, was employed in simulation of the profiles obtained at RT implantation. The introduction of such a model is necessary, since Crystal-TRIM per se can only treat ballistic processes during ion bombardment, not subsequent relaxation processes which are responsible for the formation of the final as-implanted defect structure. In the simulations, the values of the two model parameters  $C_a$  and  $p_t$  [cf. Ref. 20, Eq. (1)] were  $5.33 \text{ meV}^{-1}$

and 0.1, respectively. These data were also employed in previous investigations<sup>6</sup> of dechanneling of implanted P ions. Both parameters are used to calculate the probability that a P ion collides with an atom located within a region of an extended defect.  $C_a$  and  $p_t$  describe the increase of this probability with growing nuclear energy deposition per target atom and the onset of amorphization in the target region considered, respectively. Figure 2(a) shows good agreement between the SIMS data and the simulated profiles. The thickness of the amorphous layer calculated by Crystal-TRIM is nearly identical to the measured value. The damage buildup model was also used to simulate the low dose implants at RT. In Fig. 1(a) the gray histograms show the corresponding results. The agreement with the experimental data is better than for simulations that do not consider damage buildup. This shows that in RT implants, at a dose of about  $5 \times 10^{13} \text{ cm}^{-2}$ , defect accumulation influences slightly the shape of channeling implantation profiles. In the simulation of the P profiles obtained at elevated temperatures damage buildup is completely neglected. The good agreement with experimental data [Fig. 2(b)] demonstrates the validity of this assumption.

The results of atomistic simulations are generally consistent with the qualitative interpretation of the experimental results given above. The small deviation between simulated and measured depth profiles should mainly be due to the relatively simple models used in the simulations for electronic energy loss, lattice vibrations, and damage buildup.

The authors are grateful to Evans East, East Windsor, NJ, for the SIMS analysis. In particular they thank Dr. M. S. Denker and Dr. S. W. Novak for valuable comments.

- <sup>1</sup>G. Dearnaley, J. H. Freeman, G. A. Gard, and M. A. Wilkins, *Can. J. Phys.* **46**, 587 (1968).
- <sup>2</sup>G. Carter and W. A. Grant, *Ion Implantation of Semiconductors* (Arnold, London, 1976).
- <sup>3</sup>R. G. Wilson, *J. Appl. Phys.* **60**, 2797 (1986).
- <sup>4</sup>K. M. Klein, C. Park, and A. F. Tasch, *Nucl. Instrum. Methods Phys. Res. B* **59–60**, 60 (1991).
- <sup>5</sup>G. Hobler, *Radiat. Eff. Defects Solids* **139**, 21 (1996).
- <sup>6</sup>M. Posselt, B. Schmidt, C. S. Murthy, T. Feudel, and K. Suzuki, *J. Electrochem. Soc.* **144**, 1495 (1997).
- <sup>7</sup>E. Rimini, *Ion Implantation: Basics to Device Fabrication* (Kluwer Academic, Boston, 1995).
- <sup>8</sup>W.-K. Chu, J. W. Mayer, and M.-A. Nicolet, *Backscattering Spectrometry* (Academic, New York, 1978).
- <sup>9</sup>F. F. Morehead, Jr. and B. L. Crowder, *Radiat. Eff.* **6**, 27 (1970).
- <sup>10</sup>J. F. Ziegler, J. P. Biersack, and U. Littmark, *The Stopping and Range of Ions in Solids* (Pergamon, New York, 1985).
- <sup>11</sup>M.-J. Caturla, T. Diaz de la Rubia, L. A. Marques, and G. H. Gilmer, *Phys. Rev. B* **54**, 16683 (1996).
- <sup>12</sup>M. Posselt, *Mater. Res. Soc. Symp. Proc.* **647**, O2.1.1 (2001).
- <sup>13</sup>M. Posselt, *Radiat. Eff. Defects Solids* **130/131**, 87 (1994).
- <sup>14</sup>C. S. Murthy, M. Posselt, and T. Frei, *J. Vac. Sci. Technol. B* **14**, 278 (1996).
- <sup>15</sup>M. Posselt, B. Schmidt, T. Feudel, and N. Strecker, *Mater. Sci. Eng., B* **71**, 128 (2000).
- <sup>16</sup>O. S. Oen and M. T. Robinson, *Nucl. Instrum. Methods* **132**, 647 (1976).
- <sup>17</sup>M. Blackman, in *Handbuch der Physik*, edited by S. Flügge (Springer, Berlin, 1955), Part 1, Vol. VII, p. 327.
- <sup>18</sup>S. Datz, B. L. Berman, B. A. Dahling, M. V. Hynes, H. Park, J. O. Kephart, R. K. Klein, and R. H. Pantell, *Nucl. Instrum. Methods Phys. Res. B* **13**, 19 (1986).
- <sup>19</sup>J. O. Kephart, B. L. Berman, R. H. Pantell, S. Datz, R. K. Klein, and H. Park, *Phys. Rev. B* **44**, 1992 (1991).
- <sup>20</sup>M. Posselt, L. Bischoff, and J. Teichert, *Appl. Phys. Lett.* **79**, 1444 (2001).